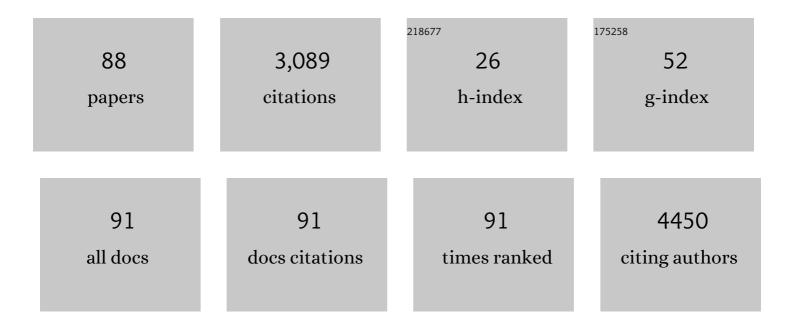
List of Publications by Year in descending order

Source: https://exaly.com/author-pdf/3739210/publications.pdf Version: 2024-02-01



VINC HUANC

#	Article	IF	CITATIONS
1	Dosimetric effect of intensity-modulated radiation therapy for postoperative non-small cell lung cancer with and without air cavity in the planning target volume. Medical Dosimetry, 2022, 47, 32-37.	0.9	0
2	Increased Combined Anteversion Is an Independent Predictor of Ischiofemoral Impingement in the Setting of Borderline Dysplasia With Coxa Profunda. Arthroscopy - Journal of Arthroscopic and Related Surgery, 2022, 38, 1519-1527.	2.7	4
3	RNA 5-methylcytosine regulates YBX2-dependent liquid-liquid phase separation. Fundamental Research, 2022, 2, 48-55.	3.3	8
4	A Metabolic Multistage Glutathione Depletion Used for Tumor-Specific Chemodynamic Therapy. ACS Nano, 2022, 16, 4228-4238.	14.6	81
5	Upregulated YB-1 protein promotes glioblastoma growth through a YB-1/CCT4/mLST8/mTOR pathway. Journal of Clinical Investigation, 2022, 132, .	8.2	21
6	What Factors Are Associated With Postoperative Ischiofemoral Impingement After Bernese Periacetabular Osteotomy in Developmental Dysplasia of the Hip?. Clinical Orthopaedics and Related Research, 2022, Publish Ahead of Print, .	1.5	4
7	Voxel-Level BED Corrected Dosimetric and Radiobiological Assessment of 2 Kinds of Hybrid Radiotherapy Planning Methods for Stage III NSCLC. Technology in Cancer Research and Treatment, 2022, 21, 153303382211079.	1.9	0
8	Deep Learning for Patient-Specific Quality Assurance: Predicting Gamma Passing Rates for IMRT Based on Delivery Fluence Informed by log Files. Technology in Cancer Research and Treatment, 2022, 21, 153303382211048.	1.9	5
9	Structural insights into dsRNA processing by Drosophila Dicer-2–Loqs-PD. Nature, 2022, 607, 399-406.	27.8	19
10	Structural basis of the bHLH domains of MyoD-E47 heterodimer. Biochemical and Biophysical Research Communications, 2022, 621, 88-93.	2.1	1
11	QKI-5 regulates the alternative splicing of cytoskeletal gene <i>ADD3</i> in lung cancer. Journal of Molecular Cell Biology, 2021, 13, 347-360.	3.3	27
12	FAM122A is required for hematopoietic stem cell function. Leukemia, 2021, 35, 2130-2134.	7.2	3
13	FAM122A promotes acute myeloid leukemia cell growth through inhibiting PP2A activity and sustaining MYC expression. Haematologica, 2021, 106, 903-907.	3.5	4
14	The complete genome of extracellular protease-producing Deinococcus sp. D7000 isolated from the hadal region of Mariana Trench Challenger Deep. Marine Genomics, 2021, 57, 100832.	1.1	4
15	Individualized Fraction Regimen of SBRT Patients With Non-Small Cell Lung Cancer Based on Uncomplicated and Cancer-Free Control Probability. Technology in Cancer Research and Treatment, 2021, 20, 153303382110119.	1.9	1
16	LOXL1 exerts oncogenesis and stimulates angiogenesis through the LOXL1-FBLN5/αvβ3 integrin/FAK-MAPK axis in ICC. Molecular Therapy - Nucleic Acids, 2021, 23, 797-810.	5.1	18
17	Horizontal Gene Transfer of Genes Encoding Copper-Containing Membrane-Bound Monooxygenase (CuMMO) and Soluble Di-iron Monooxygenase (SDIMO) in Ethane- and Propane-Oxidizing <i>Rhodococcus</i> Bacteria. Applied and Environmental Microbiology, 2021, 87, e0022721.	3.1	5
18	PS-341 alleviates chronic low-grade inflammation and improves insulin sensitivity through the inhibition of TM4 (UBAC2) degradation. Nutrition and Metabolism, 2021, 18, 54.	3.0	1

#	Article	IF	CITATIONS
19	Regression models for predicting physical and EQD2 plan parameters of two methods of hybrid planning for stage III NSCLC. Radiation Oncology, 2021, 16, 119.	2.7	2
20	Geometric and Dosimetric Changes in Tumor and Lung Tissue During Radiotherapy for Lung Cancer With Atelectasis. Frontiers in Oncology, 2021, 11, 690278.	2.8	0
21	Virtual Patient-Specific Quality Assurance of IMRT Using UNet++: Classification, Gamma Passing Rates Prediction, and Dose Difference Prediction. Frontiers in Oncology, 2021, 11, 700343.	2.8	10
22	Dosimetric comparison and biological evaluation of fixed-jaw intensity-modulated radiation therapy for T-shaped esophageal cancer. Radiation Oncology, 2021, 16, 158.	2.7	4
23	Dosimetric Comparison, Treatment Efficiency Estimation, and Biological Evaluation of Popular Stereotactic Radiosurgery Options in Treating Single Small Brain Metastasis. Frontiers in Oncology, 2021, 11, 716152.	2.8	4
24	A 2D–3D hybrid convolutional neural network for lung lobe auto-segmentation on standard slice thickness computed tomography of patients receiving radiotherapy. BioMedical Engineering OnLine, 2021, 20, 94.	2.7	6
25	Automatic segmentation of lung tumors on CT images based on a 2D & 3D hybrid convolutional neural network. British Journal of Radiology, 2021, 94, 20210038.	2.2	12
26	Rett syndrome linked to defects in forming the MeCP2/Rbfox/LASR complex in mouse models. Nature Communications, 2021, 12, 5767.	12.8	16
27	Environmental exposure to perfluoroalkyl substances in early pregnancy, maternal glucose homeostasis and the risk of gestational diabetes: A prospective cohort study. Environment International, 2021, 156, 106621.	10.0	50
28	Influence of Clinical and Tumor Factors on Interfraction Setup Errors With Rotation Correction for Vacuum Cushion in Lung Stereotactic Body Radiation Therapy. Frontiers in Oncology, 2021, 11, 734709.	2.8	0
29	lsotoxic investigation of 18F-FDG PET/CT-guided dose escalation with intensity-modulated radiotherapy for LA-NSCLC. International Journal of Radiation Biology, 2021, 97, 1-24.	1.8	0
30	Investigation of Predictors to Achieve Acceptable Lung Dose in T-Shaped Upper and Middle Esophageal Cancer With IMRT and VMAT. Frontiers in Oncology, 2021, 11, 735062.	2.8	1
31	A novel CRTâ€ i MRTâ€combined (Coâ€CRIM) planning technique for peripheral lung stereotactic body radiotherapy in pinnacle treatment planning system. Journal of Applied Clinical Medical Physics, 2021, 22, 97-107.	1.9	3
32	Account for the Full Extent of Esophagus Motion in Radiation Therapy Planning: A Preliminary Study of the IRV of the Esophagus. Frontiers in Oncology, 2021, 11, 734552.	2.8	0
33	How Does the Gradient Measure of the Lung SBRT Treatment Plan Depend on the Tumor Volume and Shape?. Frontiers in Oncology, 2021, 11, 781302.	2.8	2
34	FAM122A supports the growth of hepatocellular carcinoma cells and its deletion enhances Doxorubicin-induced cytotoxicity. Experimental Cell Research, 2020, 387, 111714.	2.6	9
35	High-throughput single-cell cultivation reveals the underexplored rare biosphere in deep-sea sediments along the Southwest Indian Ridge. Lab on A Chip, 2020, 20, 363-372.	6.0	31
36	FAM122A Inhibits Erythroid Differentiation through GATA1. Stem Cell Reports, 2020, 15, 721-734.	4.8	2

#	Article	IF	CITATIONS
37	FAM122A maintains DNA stability possibly through the regulation of topoisomerase IIα expression. Experimental Cell Research, 2020, 396, 112242.	2.6	2
38	Measuring the Ocular Morphological Parameters of Guinea Pig Eye with Edge Detection and Curve Fitting. Computational and Mathematical Methods in Medicine, 2020, 2020, 1-13.	1.3	0
39	Urban airborne PM2.5-activated microglia mediate neurotoxicity through glutaminase-containing extracellular vesicles in olfactory bulb. Environmental Pollution, 2020, 264, 114716.	7.5	36
40	Drosophila P75 safeguards oogenesis by preventing H3K9me2 spreading. Journal of Genetics and Genomics, 2020, 47, 187-199.	3.9	8
41	5-methylcytosine promotes pathogenesis of bladder cancer through stabilizing mRNAs. Nature Cell Biology, 2019, 21, 978-990.	10.3	410
42	RNA 5-Methylcytosine Facilitates the Maternal-to-Zygotic Transition by Preventing Maternal mRNA Decay. Molecular Cell, 2019, 75, 1188-1202.e11.	9.7	242
43	Single-cell CAS-seq reveals a class of short PIWI-interacting RNAs in human oocytes. Nature Communications, 2019, 10, 3389.	12.8	66
44	ER-localized Hrd1 ubiquitinates and inactivates Usp15 to promote TLR4-induced inflammation during bacterial infection. Nature Microbiology, 2019, 4, 2331-2346.	13.3	39
45	A Pandas complex adapted for piRNA-guided transcriptional silencing and heterochromatin formation. Nature Cell Biology, 2019, 21, 1261-1272.	10.3	49
46	Crystal structure of a Y-box binding protein 1 (YB-1)–RNA complex reveals key features and residues interacting with RNA. Journal of Biological Chemistry, 2019, 294, 10998-11010.	3.4	47
47	Sleep deprivation of rats increases postsurgical expression and activity of L-type calcium channel in the dorsal root ganglion and slows recovery from postsurgical pain. Acta Neuropathologica Communications, 2019, 7, 217.	5.2	16
48	Uncovering the mechanistic basis for specific recognition of monomethylated H3K4 by the CW domain of Arabidopsis histone methyltransferase SDG8. Journal of Biological Chemistry, 2018, 293, 6470-6481.	3.4	34
49	Identification of substrates of the small RNA methyltransferase Hen1 in mouse spermatogonial stem cells and analysis of its methyl-transfer domain. Journal of Biological Chemistry, 2018, 293, 9981-9994.	3.4	13
50	Vanadium(IV)-chlorodipicolinate alleviates hepatic lipid accumulation by inducing autophagy via the LKB1/AMPK signaling pathway in vitro and in vivo. Journal of Inorganic Biochemistry, 2018, 183, 66-76.	3.5	19
51	Glucocorticoids induce apoptosis and matrix metalloproteinase-13 expression in chondrocytes through the NOX4/ROS/p38 MAPK pathway. Journal of Steroid Biochemistry and Molecular Biology, 2018, 181, 52-62.	2.5	44
52	Structural insights into the sequence-specific recognition of Piwi by <i>Drosophila</i> Papi. Proceedings of the National Academy of Sciences of the United States of America, 2018, 115, 3374-3379.	7.1	18
53	Structural Insights into the pH-Dependent Conformational Change and Collagen Recognition of the Human Mannose Receptor. Structure, 2018, 26, 60-71.e3.	3.3	26
54	Structural Analysis of the Arabidopsis AL2-PAL and PRC1 Complex Provides Mechanistic Insight into Active-to-Repressive Chromatin State Switch. Journal of Molecular Biology, 2018, 430, 4245-4259.	4.2	11

#	Article	IF	CITATIONS
55	Structural and biochemical insights into small RNA 3′ end trimming by Arabidopsis SDN1. Nature Communications, 2018, 9, 3585.	12.8	23
56	Structural insights into Rhinoâ€Đeadlock complex for germline piRNA cluster specification. EMBO Reports, 2018, 19, .	4.5	19
57	Architecture of cell–cell adhesion mediated by sidekicks. Proceedings of the National Academy of Sciences of the United States of America, 2018, 115, 9246-9251.	7.1	23
58	Readers, writers and erasers of N6-methylated adenosine modification. Current Opinion in Structural Biology, 2017, 47, 67-76.	5.7	82
59	Ubiquitylation of p62/sequestosome1 activates its autophagy receptor function and controls selective autophagy upon ubiquitin stress. Cell Research, 2017, 27, 657-674.	12.0	143
60	2-Deoxy-d-Glucose Treatment Decreases Anti-inflammatory M2 Macrophage Polarization in Mice with Tumor and Allergic Airway Inflammation. Frontiers in Immunology, 2017, 8, 637.	4.8	70
61	5-HT3a Receptors Modulate Hippocampal Gamma Oscillations by Regulating Synchrony of Parvalbumin-Positive Interneurons. Cerebral Cortex, 2016, 26, bhu209.	2.9	15
62	Transcription factors AS1 and AS2 interact with LHP1 to repress <i>KNOX</i> genes in <i>Arabidopsis</i> . Journal of Integrative Plant Biology, 2016, 58, 959-970.	8.5	45
63	Structural studies on MRG701 chromodomain reveal a novel dimerization interface of MRG proteins in green plants. Protein and Cell, 2016, 7, 792-803.	11.0	6
64	Keto acid metabolites of branched-chain amino acids inhibit oxidative stress-induced necrosis and attenuate myocardial ischemia–reperfusion injury. Journal of Molecular and Cellular Cardiology, 2016, 101, 90-98.	1.9	16
65	Vanadium(IV)-chlorodipicolinate inhibits 3T3-L1 preadipocyte adipogenesis by activating LKB1/AMPK signaling pathway. Journal of Inorganic Biochemistry, 2016, 162, 1-8.	3.5	24
66	FAM122A, a new endogenous inhibitor of protein phosphatase 2A. Oncotarget, 2016, 7, 63887-63900.	1.8	26
67	Picroside II protects against sepsis via suppressing inflammation in mice. American Journal of Translational Research (discontinued), 2016, 8, 5519-5531.	0.0	4
68	Structural insights into Rhino-mediated germline piRNA cluster formation. Cell Research, 2015, 25, 525-528.	12.0	32
69	MORF-RELATED GENE702, a Reader Protein of Trimethylated Histone H3 Lysine 4 and Histone H3 Lysine 36, Is Involved in Brassinosteroid-Regulated Growth and Flowering Time Control in Rice Â. Plant Physiology, 2015, 168, 1275-1285.	4.8	31
70	Salivary uric acid as a noninvasive biomarker for monitoring the efficacy of urate-lowering therapy in a patient with chronic gouty arthropathy. Clinica Chimica Acta, 2015, 450, 115-120.	1.1	28
71	Structure of Zeste–DNA Complex Reveals a New Modality of DNA Recognition by Homeodomain-Like Proteins. Journal of Molecular Biology, 2015, 427, 3824-3833.	4.2	1
72	Rhino defines H3K9me3-marked piRNA clusters. Oncotarget, 2015, 6, 20740-20741.	1.8	1

#	Article	IF	CITATIONS
73	Regulation of Arabidopsis Flowering by the Histone Mark Readers MRG1/2 via Interaction with CONSTANS to Modulate FT Expression. PLoS Genetics, 2014, 10, e1004617.	3.5	79
74	Iron Metabolism Regulates p53 Signaling through Direct Heme-p53 Interaction and Modulation of p53 Localization, Stability, and Function. Cell Reports, 2014, 7, 180-193.	6.4	170
75	Technical Details and Clinical Outcomes of Transpopliteal Venous Stent Placement for Postthrombotic Chronic Total Occlusion of the Iliofemoral Vein. Journal of Vascular and Interventional Radiology, 2014, 25, 925-932.	0.5	56
76	Endovascular treatment for symptomatic stent failures in long-segment chronic total occlusion of femoropopliteal arteries. Journal of Vascular Surgery, 2014, 60, 362-368.	1.1	11
77	PML-RARα enhances constitutive autophagic activity through inhibiting the Akt/mTOR pathway. Autophagy, 2011, 7, 1132-1144.	9.1	37
78	Post-transcriptional regulation of miRNA biogenesis and functions. Frontiers in Biology, 2010, 5, 32-40.	0.7	6
79	Structural basis for methylarginine-dependent recognition of Aubergine by Tudor. Genes and Development, 2010, 24, 1876-1881.	5.9	117
80	Structural insights into mechanisms of the small RNA methyltransferase HEN1. FASEB Journal, 2010, 24, 499.6.	0.5	0
81	Systematic studies on the recognition of 3′â€end methylated small silencing RNAs by PAZ domains. FASEB Journal, 2010, 24, .	0.5	0
82	Structural insights into mechanisms of the small RNA methyltransferase HEN1. Nature, 2009, 461, 823-827.	27.8	129
83	Specific interaction between Lin28 and priâ€letâ€7g. FASEB Journal, 2009, 23, 844.2.	0.5	0
84	Abdominal aortic wall motion of healthy and hypertensive subjects: Evaluation of tissue Doppler velocity imaging. Journal of Clinical Ultrasound, 2008, 36, 218-225.	0.8	3
85	Detection of Small Inflammatory and Metastatic Lymph Nodes in Rabbits by Sonography. Journal of Ultrasound in Medicine, 2008, 27, 233-241.	1.7	1
86	Recognition of Histone H3 Lysine-4 Methylation by the Double Tudor Domain of JMJD2A. Science, 2006, 312, 748-751.	12.6	406
87	Crystal Structure of the HP1-EMSY Complex Reveals an Unusual Mode of HP1 Binding. Structure, 2006, 14, 703-712.	3.3	44
88	Crystallization and preliminary crystallographic study of rBmKαIT1, a recombinant α-insect toxin from the scorpionButhus martensiiKarsch. Acta Crystallographica Section D: Biological Crystallography, 2003, 59, 1635-1636.	2.5	3